



저작자표시-비영리-변경금지 2.0 대한민국

이용자는 아래의 조건을 따르는 경우에 한하여 자유롭게

- 이 저작물을 복제, 배포, 전송, 전시, 공연 및 방송할 수 있습니다.

다음과 같은 조건을 따라야 합니다:



저작자표시. 귀하는 원저작자를 표시하여야 합니다.



비영리. 귀하는 이 저작물을 영리 목적으로 이용할 수 없습니다.



변경금지. 귀하는 이 저작물을 개작, 변형 또는 가공할 수 없습니다.

- 귀하는, 이 저작물의 재이용이나 배포의 경우, 이 저작물에 적용된 이용허락조건을 명확하게 나타내어야 합니다.
- 저작권자로부터 별도의 허가를 받으면 이러한 조건들은 적용되지 않습니다.

저작권법에 따른 이용자의 권리는 위의 내용에 의하여 영향을 받지 않습니다.

이것은 [이용허락규약\(Legal Code\)](#)을 이해하기 쉽게 요약한 것입니다.

[Disclaimer](#)

**A THESIS  
FOR THE DEGREE OF MASTER OF ENGINEERING**

**Characterization of Graphene Flower based  
composites and its Electronic applications**

**Muhammad Saqib**

Department of Electronic Engineering

GRADUATE SCHOOL

JEJU NATIONAL UNIVERSITY

Febraury 2021

# Characterization of Graphene Flower based composites and its Electronic applications

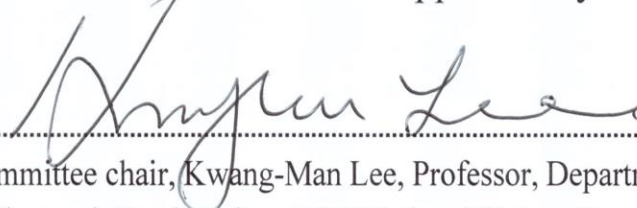
**MUHAMMAD SAQIB**

**(Supervised by Professor Woo Young Kim)**

A thesis submitted on partial fulfillment of the requirement for the degree of Master of Engineering

December 22, 2020

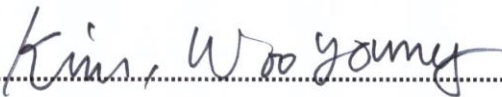
The thesis has been examined and approved by:



.....  
Thesis committee chair, Kwang-Man Lee, Professor, Department of Electronic Engineering, JEJU National University.



.....  
Kyung Youn Kim, Professor, Department of Electronic Engineering, JEJU National University.



.....  
Thesis supervisor, Woo Young Kim, Professor, Department of Electronic Engineering, JEJU National University.

**Department of Electronic Engineering JEJU National University,  
South Korea.**

## Abstract

The performance of any Electronic device has relied on the availability of suitable functional material. Like, wide band gap, high electron injection rate, easy availability, low cost, high carrier concentration, low static dielectric constant and high electron mobility are the required properties for materials to use in photovoltaic industry. Same as for other electronic devices, especially, the performance of sensors is dependent on the response of active materials used for sensing. Despite all efforts to develop new materials, it still remains a challenge to have all the desirable aspects in a single material. One of the simple, easy, and cost-effective ways to get novel functional materials with improved properties for desired applications is to make composites of selected materials.

In this work, Zinc oxide (ZnO), a transparent, wide bandgap n-type semiconductor and, a unique structure of graphene named graphene flower have been used to make a composite. A simple solution process approach has been used to make GrF/ZnO composite. GrF/ZnO composite's morphological, elemental, and structural characterizations were performed by field emission scanning electron microscope (FESEM), Energy-dispersive spectroscopy (EDS), and x-ray diffractometer (XRD), respectively.

This newly prepared GrF/ZnO composite was used as an active material for humidity sensing. An ultra-sensitive humidity sensor has been demonstrated using Graphene Flower and ZnO (GrF/ZnO) composite. The proposed humidity sensor was tested at the humidity range of 15% to 86% relative humidity RH%. The demonstrated sensor has shown a highly sensitive response to humidity, an average current change of

7.77 $\mu$ A/RH%. Also, the proposed sensor response was very stable, repeatable, ultra-fast response, and recovery time. Moreover, the demonstrated sensor was ultra-sensitive to normal human breathing, making it a promising candidate for health monitoring applications.

**Keywords: Functional material; Graphene Flower; Zinc Oxide; GrF/ZnO; solution process; Ultra-sensitive; humidity sensor; fast response & recovery time; Health monitoring.**

## Acknowledgement

I would like to thank all my colleagues and my friends at Jeju National University. I wish to extend my gratitude to my primary supervisor, Woo young Kim, and all other professors who guided me throughout this master course. I wish to acknowledge the help provided by the technical and support staff in the Electronics department of the Jeju National university.

I would also like to thank my friends and family who supported me and offered deep insight into the study.

**Muhammad Saqib**

December 1, 2020.

## 2 Abbreviations

GrF	Graphene Flower
ZnO	Zinc oxide
GrF/ZnO	Graphene flower Zinc oxide composite
FESEM	field emission scanning electron microscope
EDS	Energy-dispersive spectroscopy
XRD	X-ray diffractometer
RH%	Relative humidity
ZAD	zinc-acetate-dihydrate
MEA	monoethanolamine
IPA	isopropyl-alcohol
IDE's	interdigitated electrodes
FTO	Fluorine tin oxide
DUT	Device under test
SMU	Source measurement unit

## Table of Contents

Abstract.....	3
Acknowledgement .....	5
Abbreviations.....	6
1. Introduction.....	9
2 Fabrication and characterization of ZnO and GrF-ZnO composite.....	13
2.1 Materials.....	13
2.2 Preparation of ZnO thin films .....	13
2.3 Preparation of GrF-ZnO composite.....	14
2.4 Fabrication of humidity sensor.....	15
2.5 Device Characterization and Measurements .....	17
2.5.1 ZnO and GrF-ZnO morphology characterizations.....	17
2.5.2 EDS analysis of ZnO and GrF-ZnO.....	21
2.5.3 XRD analysis of ZnO and GrF-ZnO.....	23
3 Electrical characterization of prepared humidity sensor based on ZnO and GrF-ZnO.....	24
3.1 Experimental setup.....	24
3.2 Current response of prepared humidity sensors .....	26
3.3 Capacitance and Impedance response .....	27
3.4 Current Vs Voltage at different RH% levels.....	29
3.5 Response and Recovery of proposed sensor .....	31
3.6 Stability test.....	32



3.7	Applications .....	32
4	Comparison with previous work.....	34
4.1	Comparison of proposed work with other reported humidity sensors based on ZnO composite with graphene derivatives. ....	34
4.2	Comparison of proposed work with other reported humidity sensors based on ZnO composite with other 2D materials.....	34
4.3	General comparison of proposed work with different graphene composites-based humidity sensors. ....	35
5	Conclusion .....	37
	References .....	38

# 1. Introduction

Despite of other factors, the performance of all electronic device like photovoltaic cells, electronic displays, energy storing, energy harvesting, switching devices, sensors and actuators is mainly dependent on the functional material used for certain device. For example, wide band gap, high electron injection rate, easy availability, low cost, high carrier concentration, low static dielectric constant and high electron mobility are the required properties for materials to use in photovoltaic industry. Same as for other devices, especially, sensors performance is totally dependent on the properties of active material. For any electronic sensors, sensitivity, stability, repeatability and durability totally depends on the functional material that how fast it brings change to one of its electrical parameter resistance, capacitance, conductance or polarization etc.

Now it's looking clear that development of future electronics depends on the availability of suitable functional materials. One way to get new functional material is chemical conjugation of suitable elements. But this is a time taking, expensive, and very difficult way to get new functional material with desired properties. While, second possible, cost effective and most used route towards novel functional materials, with improved and unprecedented physical properties, is to form composites of different selected materials.

Different materials like semiconductors, insulators, metals, polymers, 2D materials and metal oxides has been widely used to make composites for various electronic applications. From different metal oxides, Zinc Oxide (ZnO) is the very important transparent wide band gap n-type semiconductor. From last two decades it is the most studied metal oxide in the field of material sciences due to its vast applications in Solar cells, optoelectronics, piezoelectricity, gas sensing, bio- applications and a lot of other

sensors. While, from the class of 2D materials, graphene, its derivatives and their verity of composites have been extensively used, for various electronic devices.

Among the different environmental factors, humidity measurement is an essential parameter for various industries like semiconductor fabs, pharmaceutical, food & beverage, agriculture, textile, refineries, paper and chemical industries, etc. [1]. The humidity sensor's importance can be realized by its market size that was valued at USD 901.7 million in 2018 and is expected to reach \$1.6 billion by 2025 [2, 3]. The relative humidity sensor is the most used from different humidity sensors and has maximum market shares [2, 3]. The relative humidity sensor can be divided into several types, depending on its operation like resistive type, a capacitive type, impedance type, field-effect transistor (FET)-type, optic-fiber type and surface acoustic wave (SAW) type, and so on [4][5][6]. Resistive, capacitive, and impedance-type humidity sensors approximately have the same device structure and are commonly used due to their facile fabrication, simplicity of operation, cost-effectiveness, and low driven power [5][7]. The performance of any type of humidity sensor is strongly dependent on functional material that can bring good change to its electrical properties w.r.t to humidity change. Currently, researchers are mainly focused on improving the humidity sensing material by preparing the new materials as well as making the composites of existing materials and therefore, several types of materials, including ceramics, polymers, biowastes, metal oxides, 2D materials, and their composites have been employed in humidity sensors [8]–[13]. Primarily, metal oxides like ZnO, SnO<sub>2</sub>, Fe<sub>2</sub>O<sub>3</sub>, CuO, and TiO<sub>2</sub> has been engaged in humidity sensing applications due to their unique electrochemical and electronic properties [14]–[17]. Among them, ZnO and its composites are widely used for humidity sensors due to its easy fabrication, low cost, high surface area, and high carrier mobility [14], [18]–[23]. Different structure of ZnO, including nanowires,

nanorods, nanoparticles, and thin films has been used to improve sensor sensitivity, response time, recovery time, and other essential factors [24]–[28]. However, humidity sensors based on pure ZnO are deficient in sensitivity and have low response/recovery time, limiting their practical applications. Therefore, ZnO composites with a different type of materials like metals, semiconductors, polymers, ceramics, and 2D materials have been used by many researchers to improve its humidity sensing properties [16], [18]–[23].

The composite of ZnO with different 2D materials like graphene, MoS<sub>2</sub>, and WS<sub>2</sub> was investigated and shown great response to humidity due to the high surface to volume ratio, large surface area, and improved chemical and electrical properties of composites [29]–[31]. Among these 2D materials, graphene got great attention due to its excellent properties like high conductivity, the large specific surface area of 2600 m<sup>2</sup> g<sup>-1</sup>, optically transparent and high chemical stability. Therefore, graphene and its derivative composites are widely investigated for humidity sensor like SnO<sub>2</sub>/RGO [32], Methyl red/Graphene flakes [33], BP/graphene [34], lignosulfonate/RGO [35], BP/GO [36], Non-woven fabric/GO [37], Orange die and graphene composite [38], graphene/PVA/SiO<sub>2</sub> [39], chitosan and graphene quantum dots composites [40] and much more [6]. Especially, different forms of graphene and its derivatives have been used to improve the humidity sensing performance of ZnO, like Graphene flakes/ZnO [29], Graphene foam/ZnO [41], Graphene quantum dot/ZnO nanowires [42], ZnO/PVP-RGO [43] and Zinc Oxide/Graphene Oxide [44], etc. Still improvement in long-range, stable, more sensitive, fast response and recovery time and easy to fabricate humidity sensor is needed.

Herein, we proposed a simple approach to fabricate and characterize the humidity sensor based on graphene flower, a type of graphene that is directly synthesized based

on high rate CVD method using a bottom-up system) ZnO thin film composite. The proposed sensor showed a swift response time of a few milliseconds and a recovery time of 3 seconds, excellent stability, and sensitivity to long-range RH%. ZnO thin film was grown by the sol-gel method, and the graphene flower was spray coated on ZnO thin film. GrF/ZnO composite was characterized by field emission scanning electron microscope FESEM, Energy-dispersive spectroscopy EDS, and X-ray diffractometer XRD. The prepared sensor's electrical response has been measured by LCR meter and Precision Source Measurement unit at different RH% levels.

The aim of this thesis is to develop a composite of a special structure graphene named as graphene flower and ZnO (GrF-ZnO composite) for humidity sensing applications.

In chapter 2, synthesis of ZnO and GrF-ZnO composite, and used experimental setup is discussed. ZnO and GrF-ZnO composite was characterized by different techniques, their results are also discussed in this chapter.

Chapter 3, is describing the electrical response of fabricated composite based humidity sensors. Its sensitivity, stability response/ recovery and practical applications are also discussed in this chapter.

At the end of thesis, a broad comparison of this fabricated humidity sensor with other reported result is discussed.

## 2 Fabrication and characterization of ZnO and GrF-ZnO composite

### 2.1 Materials

For the preparation of ZnO and GrF-ZnO composite, zinc-acetate-dihydrate (ZAD), monoethanolamine (MEA), ethanol isopropyl-alcohol (IPA), acetone, and DI water was purchased from Sigma-Aldrich South Korea. Graphene Flower (GrF) solution in MEK (99.9wt%) was purchased from InALA Japan; all materials were used without modification. While glass substrate and silver paste for electrode preparation were purchased from MTI Korea.

Nine types of different salts LiCl, CH<sub>3</sub>COOK, CaCl<sub>2</sub>, K<sub>2</sub>CO<sub>3</sub>, NaBr, CuCl<sub>2</sub>, NaCl, KCL, and K<sub>2</sub>SO<sub>4</sub> were purchased from DAEJUNG Materials Korea to make supersaturated solutions to achieve different RH% levels.

### 2.2 Preparation of ZnO thin films

Simple sol-gel method was used to make ZnO thin films. Fabrication steps are shown in Figure 1. The glass was used as a substrate; first, it was cleaned by acetone, isopropanol, and DI water each for 30 minutes sonication Figure 1(a). Before depositing, the ZnO layer substrate was cleaned by UV-ozone treatment as Figure 1(b). For the preparation of ZnO thin films, an optimum study for the best molar solution of ZAD has been performed by using three different molar solutions 1M, 0.5M, and 0.1M of ZAD in ethanol, and it's found that 0.5M solution gives the best results compared to other solutions. 0.1M need a greater number of times spin coating to get the desired thickness. In contrast, thin-film is not achievable by 1M solution because that was very dense.

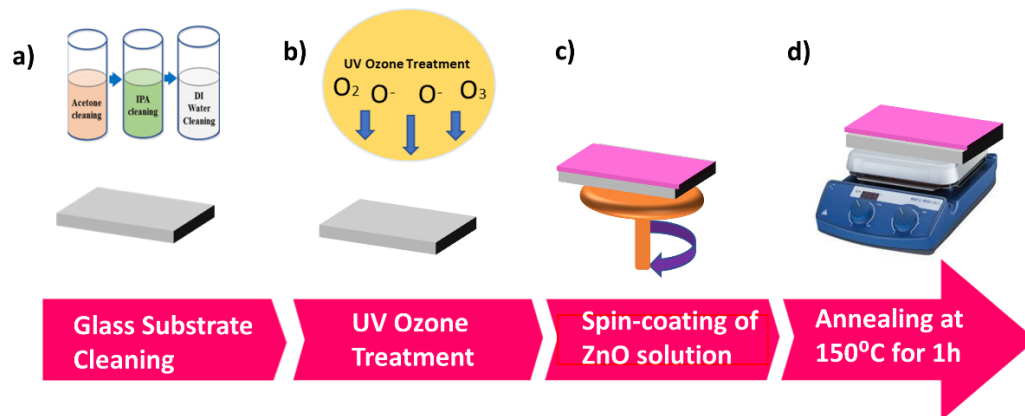


**Figure 1. ZnO thin film preparation method; a) Substrate cleaning; b) UV-ozone treatment; c) Sol-gel ZnO thin film deposition; d) Annealing for 1 hour.**

After UV-Ozone cleaning of glass substrate 0.5M solution of ZAD and MEA in ethanol was two-step spin-coated (500 rpm for 30 Sec and 1500 rpm for 15 Sec) heated at 150°C for 20 minutes and repeated for seven-time to get a uniform thin film, Figure 1(c) at the end annealed for one hour The uniform ZnO thin films can be achieved by multiple number of spin-coatings, many authors reported different number of spin-coatings [1]–[3] to get uniform ZnO thin film. In this work, optimized study has been done, and we found that minimum seven times spin-coating is required to get a smooth ZnO thin film. After that, the sample was heated at 150°C for one hour on hotplate Figure 1(f).

## 2.3 Preparation of GrF-ZnO composite

For the preparation GrF-ZnO composite only one step was extra from the ZnO thin film synthesis. Same step was followed i.e. glass substrate cleaning, UV ozone cleaning, ZAD solution spin-coating. In the last step solution of graphene flower was spray coated and annealed at 150°C for 1 hour. Figure 2, is showing the synthesis steps for GrF-ZnO composite.

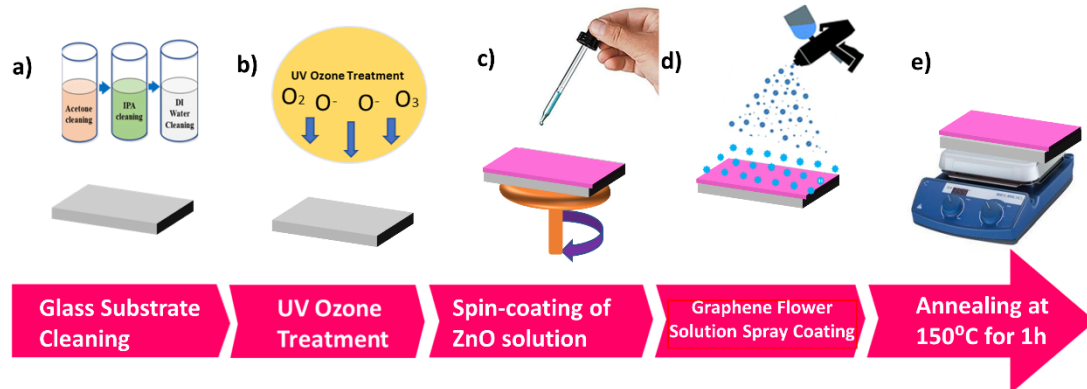


**Figure 2. GrF-ZnO composite preparation flow diagram; a) Substrate cleaning; b) UV-ozone treatment; c) Sol-gel ZnO thin film deposition; d) Spray coating of GrF solution e) Annealing for 1 hour.**

## 2.4 Fabrication of humidity sensor

Fabrication steps are shown in Figure 3. The glass was used as a substrate; first, it was cleaned by acetone, isopropanol, and DI water each for 30 minutes sonication Figure 1(a). Secondly, interdigitated electrodes (IDE's) were fabricated on this cleaned glass using screen printing method Figure 1(b). Before depositing, the active GrF/ZnO layer substrate was cleaned by UV-ozone treatment as Figure 1(c). For the preparation of ZnO thin film, an optimum study for the best molar solution of ZAD has been performed by using three different molar solutions 1M, 0.5M, and 0.1M of ZAD in ethanol, and it's found that 0.5M solution gives the best results compared to other solutions, 0.1M need more number of times spin coating to get the desired thickness. In contrast, thin-film is not achievable by 1M solution because that was very dense. After UV-Ozone cleaning of IDE's 0.5M solution of ZAD and MEA in ethanol was two-step spin-coated (500 rpm for 30 Sec and 1500 rpm for 15 Sec) heated at 150°C for 20 minutes and repeated for seven-time to get a uniform thin film, Figure 1(d) at the



end annealed for one hour [45][46]. In the next step, the GrF solution in MEK solvent was spray coated on that ZnO spin-coated film Figure 1(e); after that, the sample was heated at 150°C for one hour on hotplate Figure 1(f).

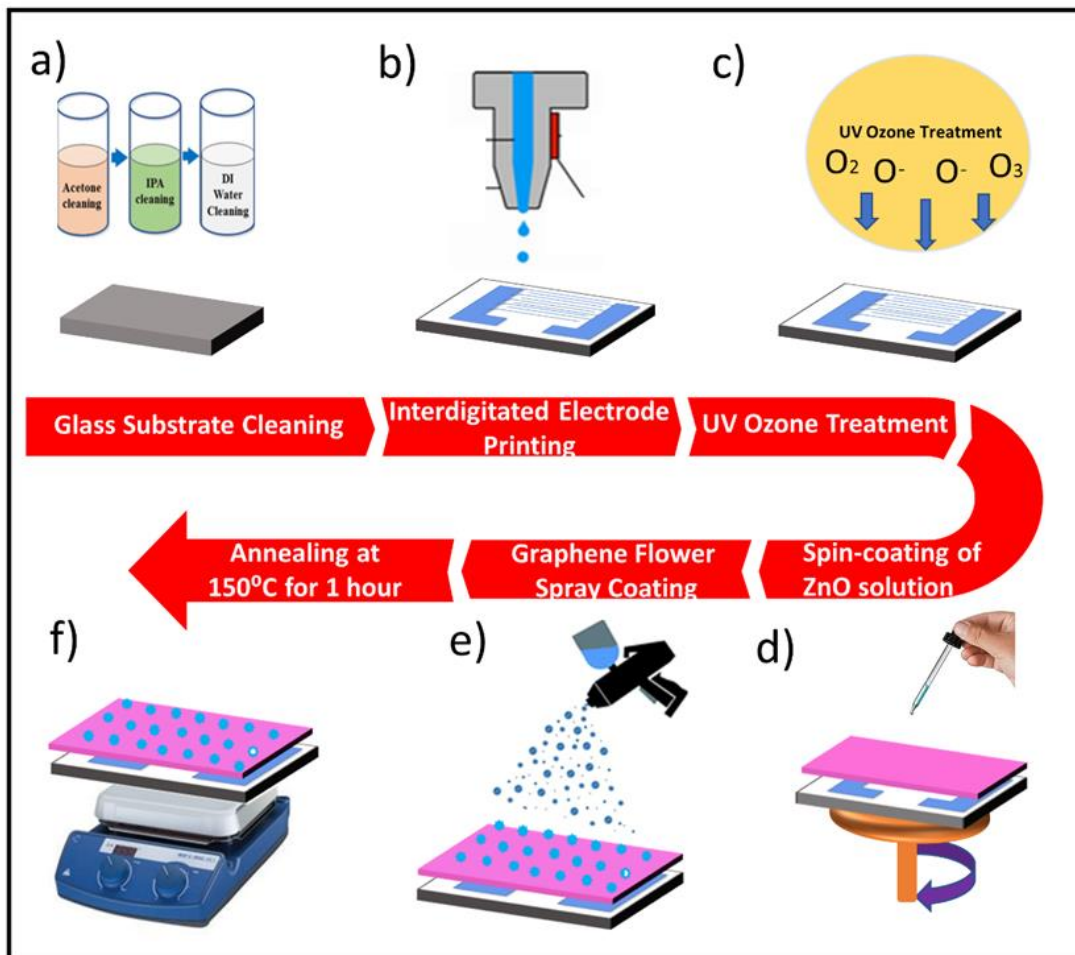


**Figure 3. Process flow diagram; a) Substrate cleaning; b) Electrode printing; c) UV-ozone treatment; d) Sol-gel ZnO thin film deposition; e) GrF spray coating; f) Annealing for 1 hour.**

## 2.5 Device Characterization and Measurements

The morphology of ZnO thin film and GrF/ZnO composite was investigated by field emission scanning electron microscope (TESCAN MIRA3), and electrode printing was confirmed by microscope (Olympus BX60). Figure 4, shown the microscopic image that mentions the finger width and distance between two fingers; also, the camera picture of printed interdigitated electrodes on the glass substrate is shown in Figure 4. Energy-dispersive spectroscopy (EDS) was used for the elemental analysis of prepared composite films. Phase analysis of ZnO and GrF/ZnO composite thin film was performed by X-ray diffractometer (Empyrean) using Cu target at the wavelength of 1.5406 Å, step size 0.02° and scanning range from 5° to 80°.

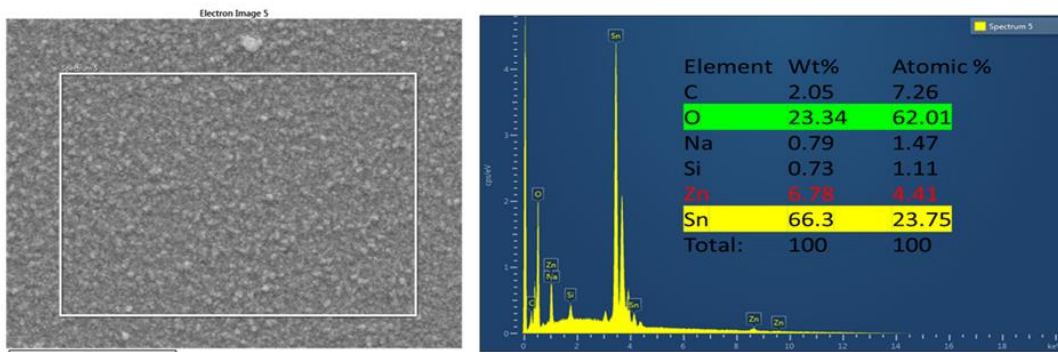


**Figure 4, Microscopic and camera image of screen-printed interdigitated electrodes.**

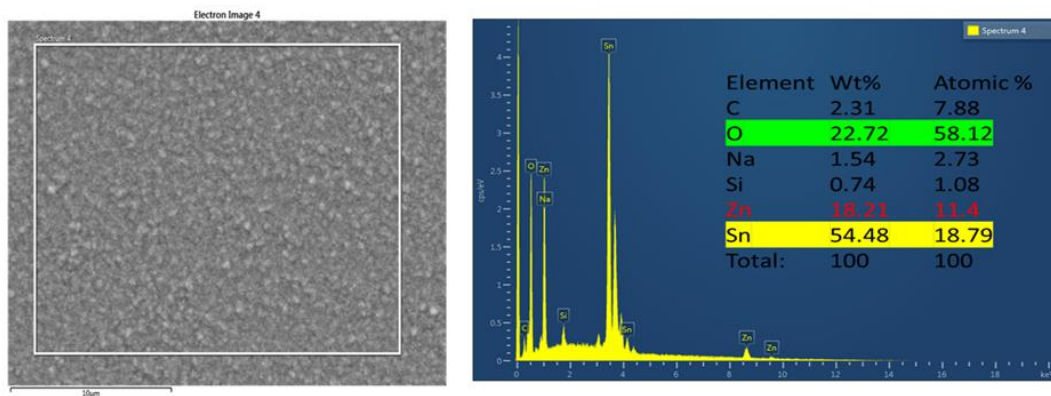
### 2.5.1 ZnO and GrF-ZnO morphology characterizations

FESEM is used to examine the morphology of ZnO and GrF/ZnO thin film. For the uniform thin film of ZnO by the sol-gel method, multiple spin coatings are required [46], [47]. Therefore, a detailed study has been done to find the effect of the different spin coatings on ZnO thin film, samples with 1,3,5,7,9 and 11 number of spin-coating were analyzed, FESEM and EDS analysis results are shown in Figure 5. It demonstrated that a minimum of seven times of spin coating gives a uniform thin film of ZnO, while more than seven-time of spin coating approximately gives the same thin film as for

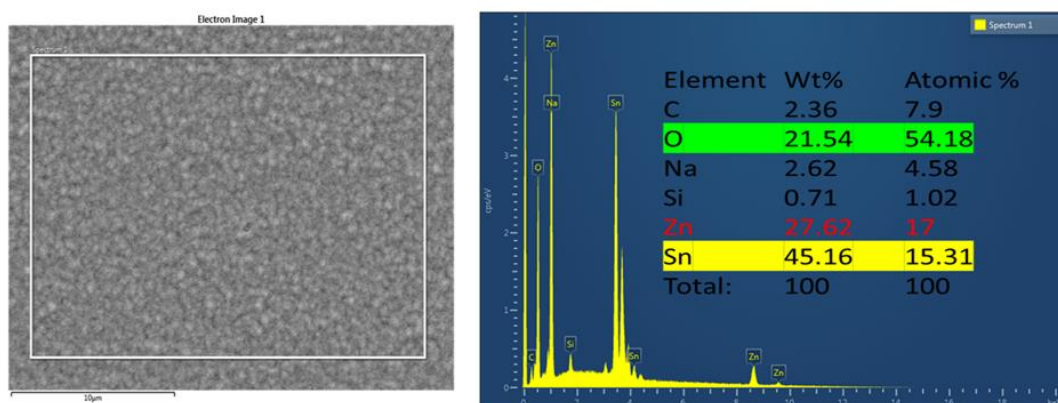
seven-time spin coating and below seven-time gives a nonuniform, i.e., different on center and corners.



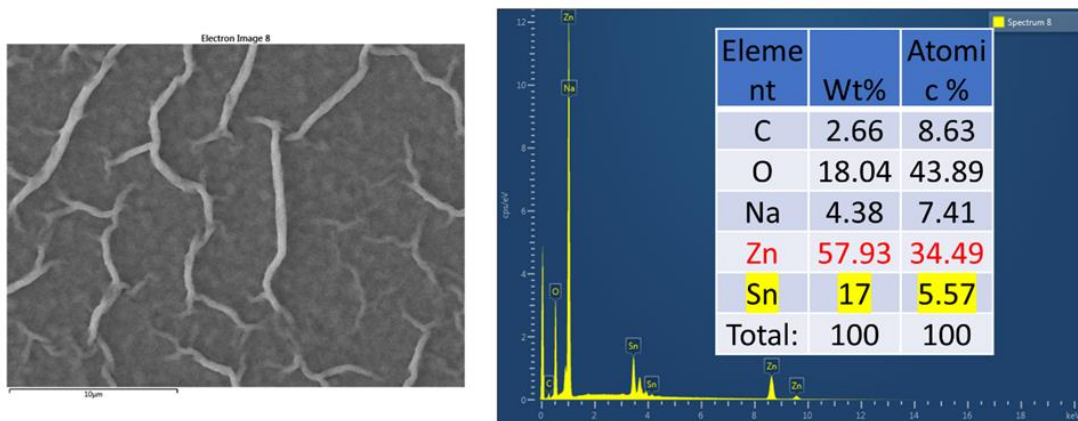
FESEM and EDS analysis of one time spin-coated ZnO thin film



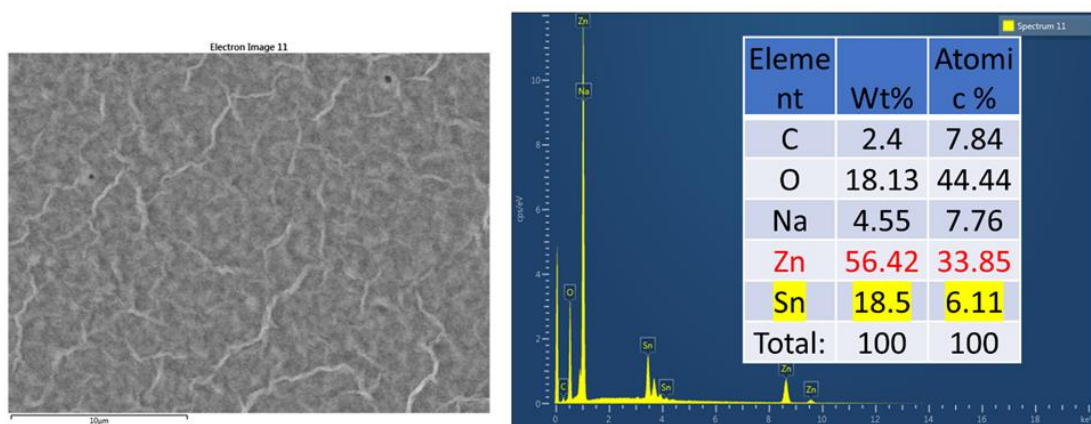
FESEM and EDS analysis of three time spin-coated ZnO thin film



FESEM and EDS analysis of five time spin-coated ZnO thin film



FESEM and EDS analysis of 7 times spin-coated ZnO thin film.



FESEM and EDS analysis of 9 times spin-coated ZnO thin film.

**Figure 5, A detailed FESEM and EDS analysis of ZnO thin film**

Figure 5, is showing an optimized analysis of ZnO thin film grown by sol-gel method, it is illustrating the effect of different number of spin-coatings on the morphological and elemental properties of ZnO thin films. The uniform ZnO thin films can be achieved by multiple number of spin-coatings, many authors reported different number of spin-coatings [1]–[3] to get uniform ZnO thin film. In this work, optimized study has been done, and we found that minimum seven times spin-coating is required to get a smooth ZnO thin film.

Figure 6(a, b, and c) illustrate the surface morphology of the optimized ZnO thin film; it revealed that ZnO has a relatively smooth surface. Figure 6(d, e, and f) is viewing the morphology of GrF/ZnO composite, which clearly shows that it has pores morphology and greater surface area compared to pristine ZnO thin film. FESEM results confirmed that GrF/ZnO composite has a high surface area to volume ratio and highly pores morphology essential for any material to be an excellent active layer for humidity sensing.

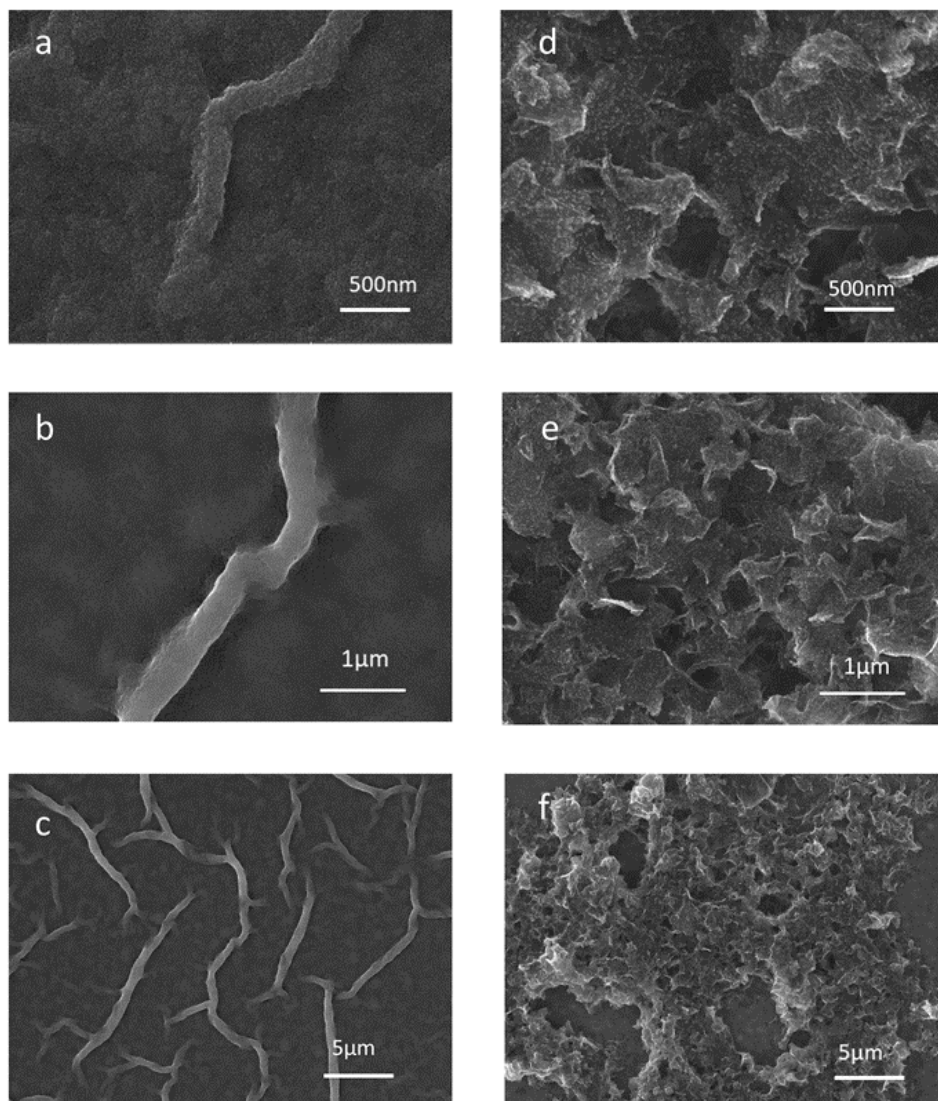


**Figure 6. FESEM analysis of grown thin films, (a, b and c) SEM images of ZnO thin film on different magnification; (c, d, and f) GrF/ZnO composite SEM images on various magnification.**

## 2.5.2 EDS analysis of ZnO and GrF-ZnO

EDS analysis has usually used to confirm the elemental composition of the given samples; therefore, EDS analysis was performed to verify the synthesis of ZnO and GrF/ZnO thin films. Samples were made on fluorine tin oxide (FTO) coated glass to perform EDS analysis. EDS of FTO glass, ZnO thin film, and GrF/ZnO are shown in Figure 7 (a, b, and c). It is clearly shown in the EDS spectrum of FTO glass Figure 7(a) that tin (Sn) and oxygen are the only dominant elements with wt% of 73.66% and 23.43%, respectively. Figure 7(b) illustrates the EDS spectrum of ZnO thin film deposited on FTO glass by the sol-gel method; it is confirming that ZnO thin film is grown successfully as zinc (Zn) was present in the spectrum with wt% of approximately 60%. Synthesis of GrF/ZnO was also confirmed by EDS analysis Figure 7 (c), showing the presence of carbon (C), zinc (Zn) oxygen (O), and tin (Sn) in the wt% of 21%, 15%, 36%, and 25% respectively.

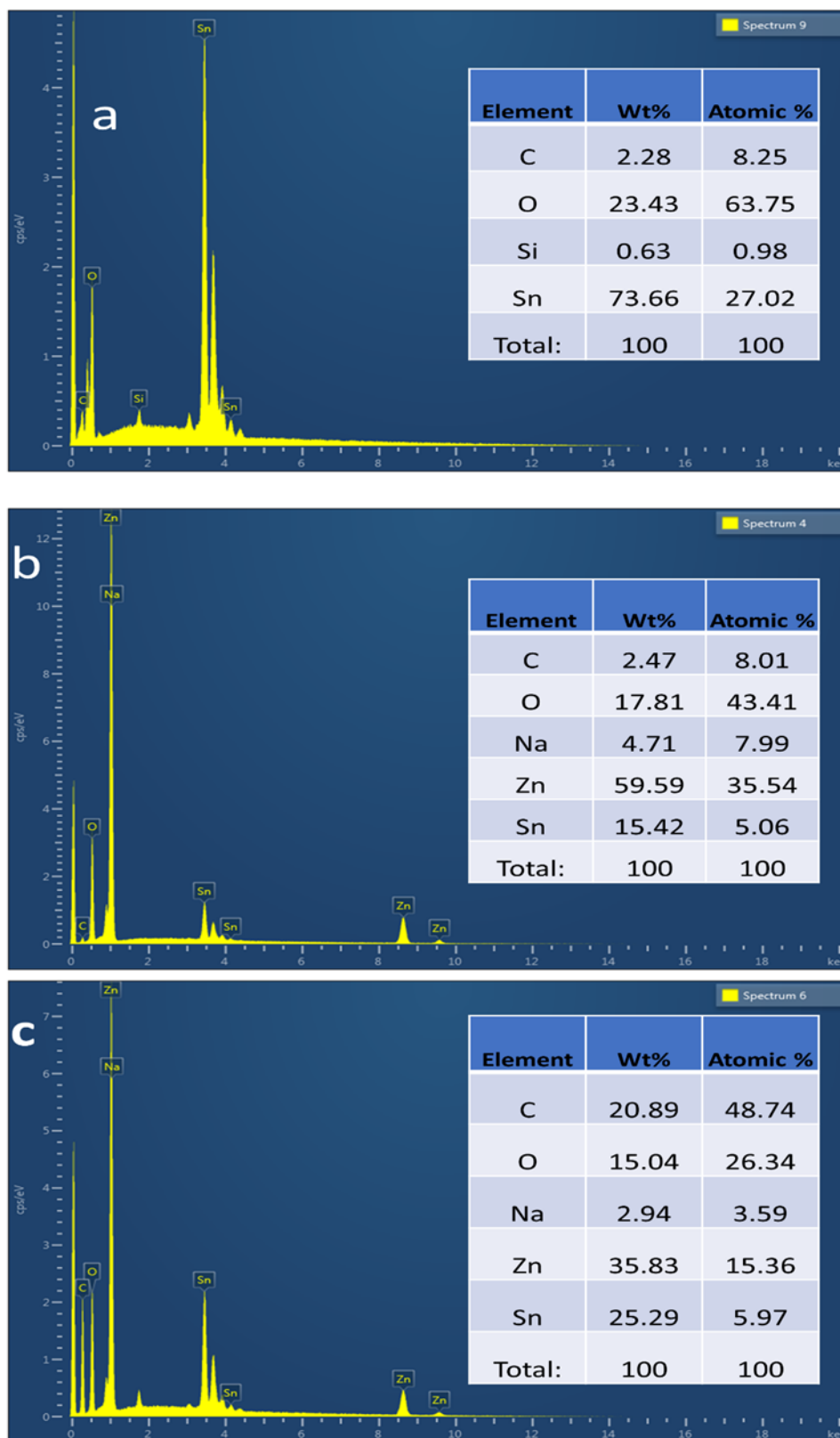


**Figure 7. EDS analysis of, (a) EDS spectrum of FTO glass (that was used as a substrate); (b) EDS spectrum of ZnO thin film; (c) GrF/ZnO composite.**

### 2.5.3 XRD analysis of ZnO and GrF-ZnO

XRD analysis was performed to investigate the crystal structure of prepared ZnO and GrF/ZnO thin films using the X-ray diffractometer (Empyrean) at a step size of  $0.02^\circ$  from  $5^\circ$  to  $80^\circ$ . XRD analysis of ZnO thin film shown the peaks at  $31.7^\circ$ ,  $34.4^\circ$ , and  $36.4^\circ$  Figure 8(a), which are corresponding to lattice planes (100), (002) and (101) respectively that confirm the hexagonal wurtzite structure of ZnO thin film according to JCPDS card no. 36-1451 and also according to the literature [47]. In Figure 8(b), XRD analysis of GrF/ZnO composites is given and shown the extra peak at  $2\theta=26^\circ$ , which is corresponding to (002) lattice plane of graphene [48], [49] and peaks at  $31.7^\circ$ ,  $34.4^\circ$ , and  $36.4^\circ$  are corresponding to lattice planes (100), (002) and (101) of ZnO respectively.

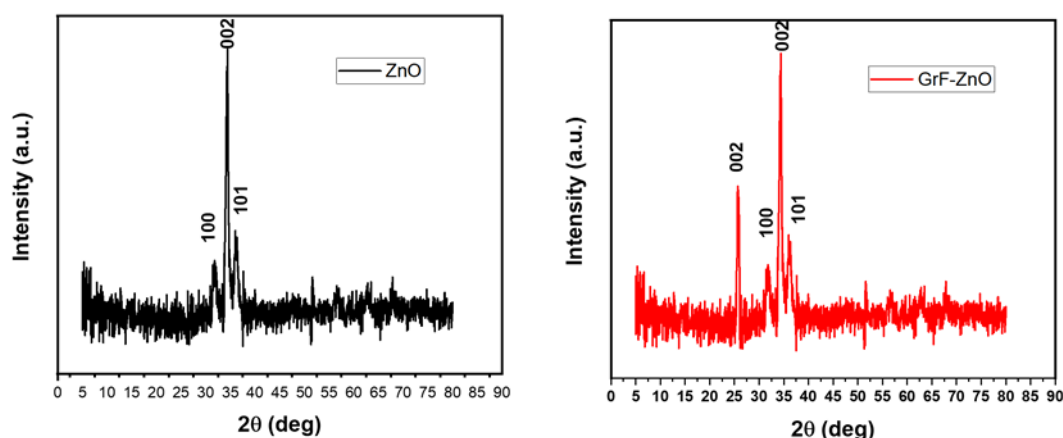


Figure 8. XRD analysis of (a) ZnO thin film; (b) GrF/ZnO composite.



### 3 Electrical characterization of prepared humidity sensor based on ZnO and GrF-ZnO.

#### 3.1 Experimental setup

The experimental setup is shown in Figure 9; a supersaturated solution of different salts has been used to achieve various RH% levels in airtight glass jars to examine sensor response to humidity. In literature[9], [36], the reported RH% level of different salt super-saturated solution are lithium chloride (11%), potassium acetate (23%), calcium chloride (33 %), potassium carbonate (43%), sodium bromide (57%), sodium chloride (67%), copper chloride (87%) and potassium sulfate (97%) but we achieved minimum RH% of 15% by LiCl and maximum RH% of 86% from K<sub>2</sub>SO<sub>4</sub> super-saturated solution. To calibrate the humidity level of supersaturated solutions, a commercially available humidity sensor, HTU21D, was used along with an Arduino board. The device under test (DUT), i.e., the fabricated sensors, was placed in the desired RH% environment by placing the DUT to the corresponding salt solution jar for electrical measurements w.r.t humidity.

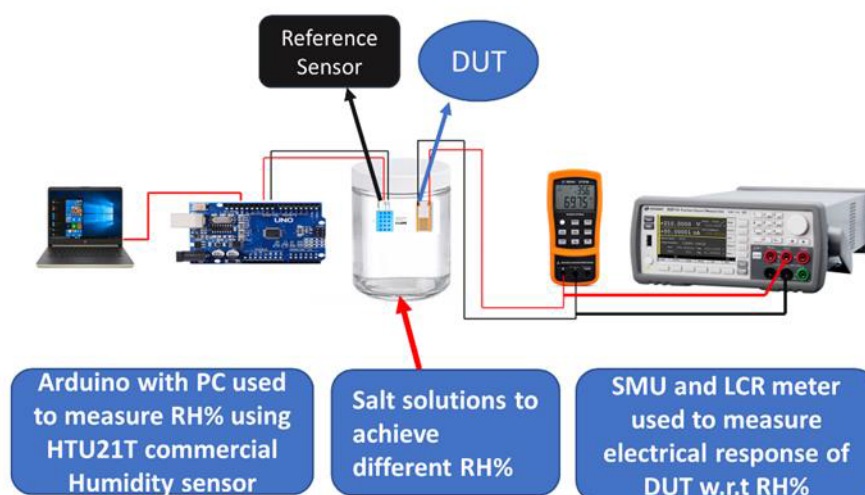


**Figure 9. Experimental setup used for Electrical measurement of DUT.**

Salt solution	LiCl	CH <sub>3</sub> COOK	CaCl <sub>2</sub>	K <sub>2</sub> CO <sub>3</sub>	NaBr	CuCl <sub>2</sub>	NaCl	KCL	K <sub>2</sub> SO <sub>4</sub>
RH%	15%	23%	32%	46%	60%	67%	72%	80%	86%

**Table 1. RH% achieved in the airtight jar by the supersaturated solution of different salts.**

Change in electrical properties of demonstrated sensor w.r.t to RH% was measured with different electronic devices, LCR meter (KEYSIGHT U1733C) was used to measure impedance response of sensors w.r.t different RH% levels. While, precision source measurement unit (KEYSIGHT 2911A) was used to measure current change w.r.t RH%, response and recovery time, the stability of devices, and different application tests of the proposed humidity sensor. The picture of the used setup is shown in Figure 10.



**Figure 10, Setup used for measuring electrical response w.r.t RH%.**

### 3.2 Current response of prepared humidity sensors

The setup shown in Figure 9, was used to measure the proposed sensor's electrical response w.r.t relative humidity. The different salt solution has been used to achieve various RH% levels, minimum RH% of 15%, and maximum RH% of 86% was achieved using supersaturated solutions of LiCl and K<sub>2</sub>SO<sub>4</sub>, respectively. A biased voltage of 3V was given to fabricated sensors using KEYSIGHT B2911A Precision Source/ Measure Unit, and the current has been measured by placing the sensor to different RH% levels. Figure 11(a) shown the current change w.r.t RH%, GrF/ZnO composite based device shown the numerous current changes over RH% humidity, as RH% increases from 15% to 86% current changes from few nanoamps to hundreds of microamps. Due to the change in conductivity of GrF/ZnO composite w.r.t RH%, increasing RH% more water vapors absorbed by the active layer and incredibly high specific surface area materials just like Graphene Flower, that increase tendency to absorb water vapors and in the result their conductivity increases. These results were according to our expectation because Graphene Flowers's surface area rich particles increase the overall surface area and conductivity of ZnO thin film. Hence, as humidity increases, more water vapors are absorbed, and more current was passed. Also, these results are following many graphene-based humidity sensors reported in the literature [4], [29], [36], [41], Smith et al. [4] said a decrease in resistance of graphene sheet as humidity increases, S. Ali et al. [33] shown that resistance of graphene flakes/ methyl red composite was decreased as RH% increases. Moreover, as shown in Figure 11(a), a pristine ZnO-based device shown random current change over the RH% change; initially, the change is approximately zero, whereas, after 60% RH, it brings a sharp change. While, GrF/ZnO based humidity sensor has shown a better current change over

the whole RH range as compare to pristine ZnO based humidity sensor, Figure 11(b).

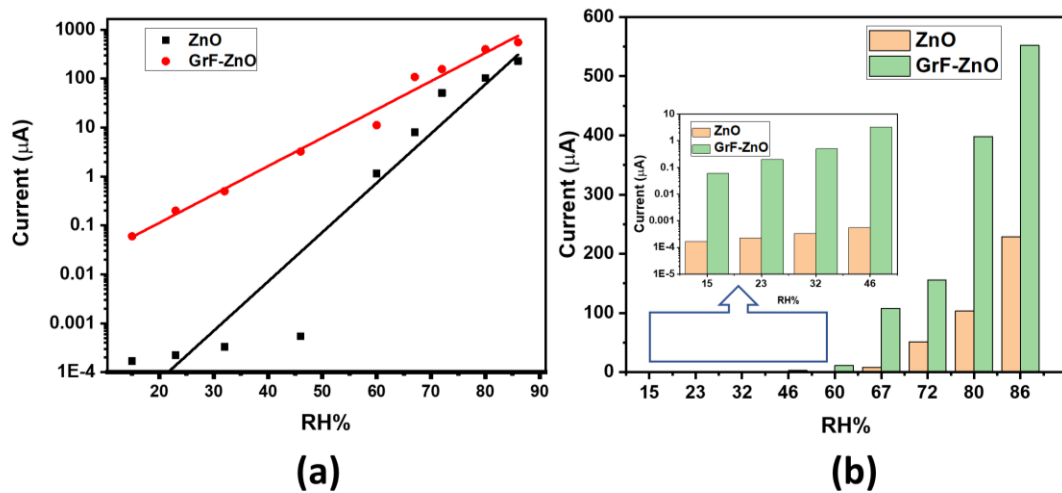


**Figure 11. Electrical response w.r.t RH%, (a) Current vs RH%; (b) Comparison of current at different RH% {inset is showing the current comparison for low humidity levels}.**

### 3.3 Capacitance and Impedance response

Similarly, as current change over RH% was measured, Impedance and capacitance change w.r.t RH% was measured using KEYSIGHT U1733C LCR meter ( $V_o = 0.7\text{ V}$  at different test frequencies of 1kHz, 10kHz and 100kHz). Figure 12, showing the capacitance response w.r.t RH% for GrF/ZnO based humidity sensor, as RH% increase the capacitance also increases. The impedance response at different levels of relative humidity for sensor was recorded. The water content in the humid environment affected sensing layer of the composite material and it was recorded at different frequencies as shown in the Figure 8. The measured result clearly shows that the normalized impedance of sensor under test increases with increase in relative humidity. This behavior is consistent at 1KHz, 10 KHz and 100 KHz for sensing device. As increasing RH%, impedance decreases this result cross verify the previous current vs. RH% result

i.e. decreasing impedance means current will increase, also according to prior reported results [4], [36], [41].

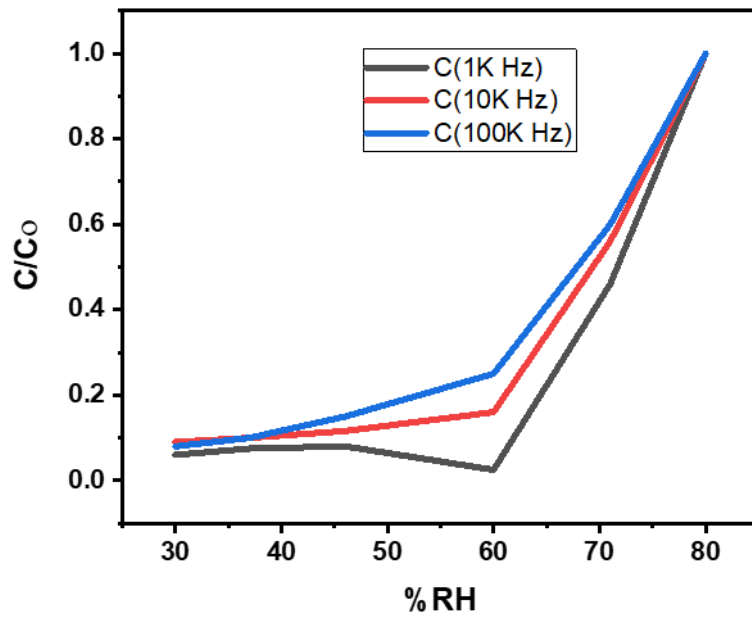


**Figure 12, Normalized capacitance response of GrF/ZnO based humidity sensor at different frequencies.**

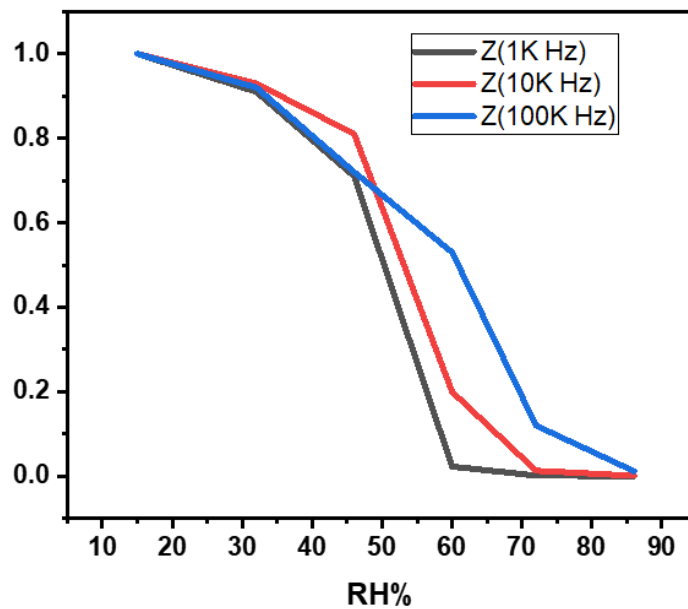


**Figure 13, Normalized impedance response of GrF/ZnO based humidity sensor at different frequencies.**

The decrease in impedance phenomenon can be explained using electronic conduction occurred due to increase of water content in the composite film. This fabricated sensing device has a very large impedance and this impedance can be decreased if the graphene nanoparticles are electrically connected to each other by anyway like through the absorption of water vapors. Hence ZnO blended graphene flowers play a key role in creating electrical connections between them. And the absence of water molecules will result in the increase of impedance. So, when the water molecules reach the surface of sensing layer, polymer film absorbs these vapors causing electrical connection between graphene flower nanoparticles and decreasing the sample resistance.

### 3.4 Current Vs Voltage at different RH% levels

Figure 14, depicted the current over voltage response of both pristine ZnO and GrF/ZnO based devices placing in a particular RH% level. The device was placed in desire RH% level jar initially for 20 minutes to stabilize the closed jar's humidity. Then, voltage sweep from 0 to 3 volts has been given by KEYSIGHT B2911A Precision Source/ Measure Unit (interfaced with PC), and the current was measured correspondingly. These results confirm the ohmic behavior of the proposed device and cross verify the previous results of increasing current with increasing RH% because as moved from 15% to 86% relative humidity levels, current level is also increased Figure 7(a-d). As clearly shown in Figure 14(a-d), the GrF/ZnO based device has established a tremendous current change w.r.t voltage sweep at each RH% level that confirms its ohmic behavior and the possibility of operation at low voltages. While pristine ZnO device has approximately zero current change w.r.t voltage sweep at low humidity levels, Figure 14(a, b), and low current change at high RH% levels compared to GrF/ZnO based device, Figure 14(c, d). These results favor of GrF/ZnO based device

in respect of operation power that GrF/ZnO based device required less power than pristine ZnO based devices.

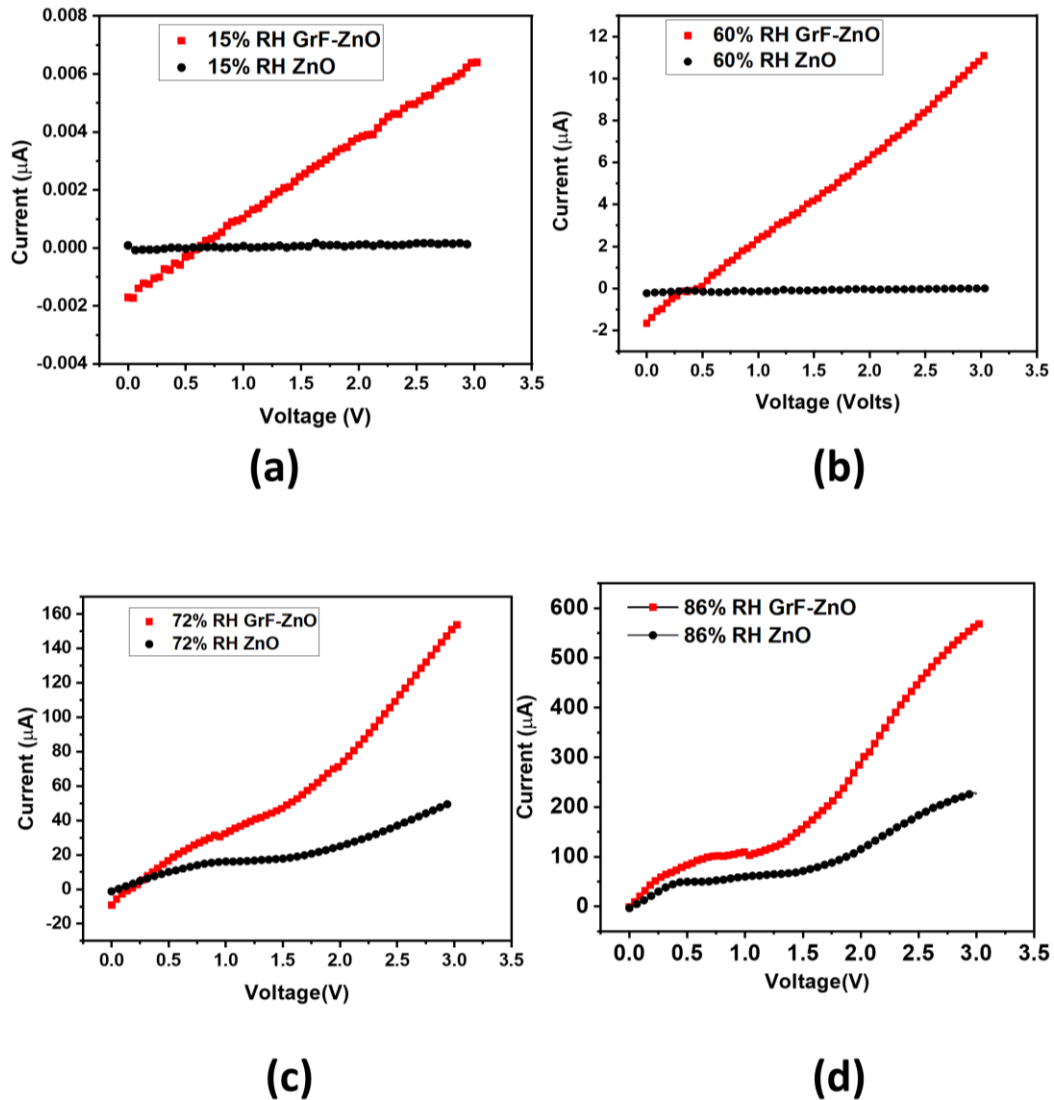


**Figure 14. Current vs Voltage at different RH%, (a) 15% RH; (b) 60% RH, (c) 72% RH and (d) 86% RH.**

### 3.5 Response and Recovery of proposed sensor

Response and recovery time are the essential features for any humidity sensor, and these are the main characteristics based on which sensors' performance is decided. Response and recovery time of proposed sensor (GrF/ZnO as an active layer) was measured. Changing sensor from one jar (low-level RH%) to another jar (high-level RH%) takes few minutes; therefore, response and recovery time measurement using this setup was not possible, so an alternate method was used. Using KEYSIGHT B2911A Precision Source/ Measure Unit, a bias voltage of 3V was applied to the fabricated sensor, and humidifier output (Humid air) was applied to the sensor's surface. The corresponding current change was measured by KEYSIGHT B2911A Precision Source/ Measure Unit. Figure 15, is showing the response and recovery time graph; our proposed sensor has shown a very fast response (0.4 Sec) to humid air as well as so short recovery time of just 4 Second, these results are so fast as compare to other reported results graphene sheet [4],[29],[42].

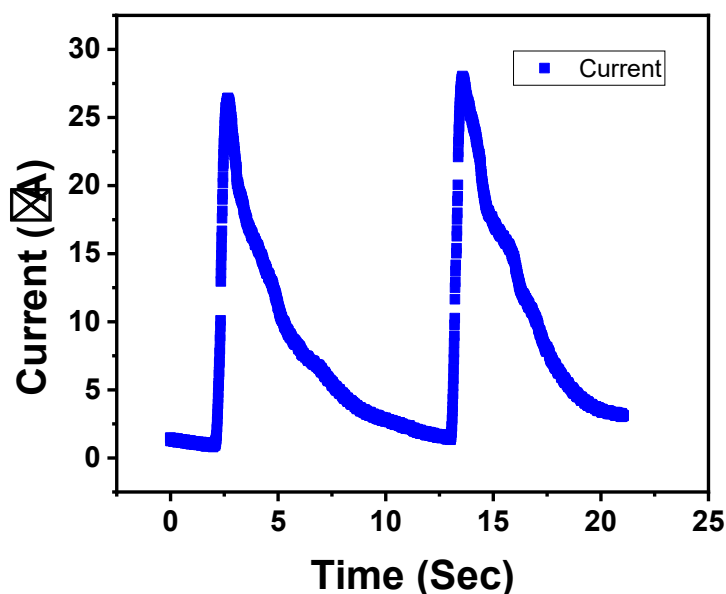


Figure 15. Response and recovery time of proposed humidity sensor.



### 3.6 Stability test

For any type of sensor, stability is an important requirement; the fabricated sensor's stability has been measured by placing the sensor in different RH% level jars, applying a bias voltage of 3V, and measuring the corresponding current continuously for 1 hour. Figure 16, showing the stability result of the demonstrated GrF/ZnO based humidity sensor. The fabricated sensor has been placed in 15%, 46%, 60%, 72%, and 86% RH jars, and continuously current was measured, as shown in Figure 16, sensor give a constant current value at every RH% level.

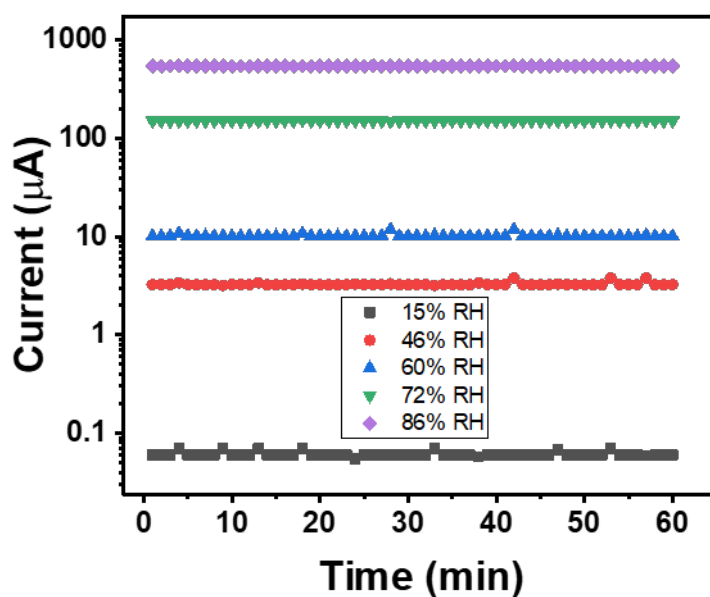


Figure 16. stability test of proposed sensor, time vs current.

### 3.7 Applications

Human breathing also contains water vapors, and it can be measurable by humidity sensor, as our proposed sensor has shown a fast response and recovery time and has the capability of measuring the rapid and small RH% change. The sensor response over normal breathing was tested. Figure 17, depicted the change of current w.r.t normal

human breathing. As the air was exhaled from the mouth, it contained the water vapors; due to these water vapors' conductivity of active layer increases and more current was passed and measured, during inhaling conductivity decreases. This proposed sensor showed an excellent response to breathing. The current change was in the microamps range; therefore, this proposed sensor can be a promising candidate for health monitoring applications.

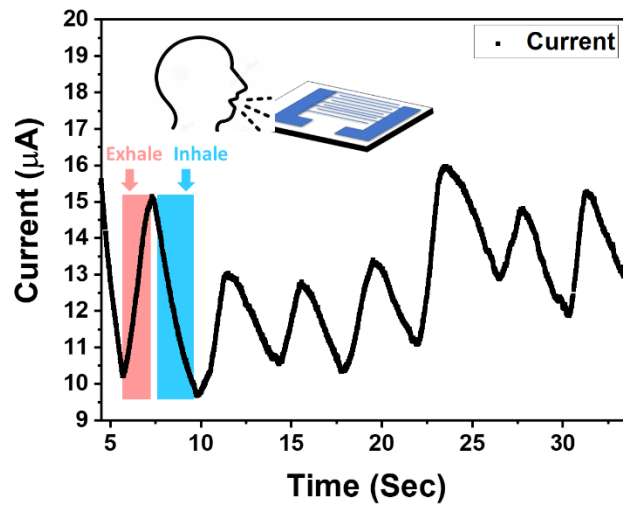


Figure 17. Sensor response to normal human breathing.

## 4 Comparison with previous work

### 4.1 Comparison of proposed work with other reported humidity sensors based on ZnO composite with graphene derivatives.

Graphene and its derivatives composites with ZnO have been reported by many authors for humidity sensing applications. Table 2 compares this demonstrated work with different reported humidity sensors, using ZnO composites with different types of graphene or its derivatives. This comparison table clearly shows that this proposed sensor has very fast response and recovery time and is highly sensitive to humidity compared to other ZnO/Graphene composites.

Active material	Response Time (Sec)	Recovery Time (Sec)	Sensitivity (X/%RH)	Range	Reference
ZnO/GrF	0.4	4	7.7 $\mu$ A/%RH	15%-86%	This Work
ZnO NWs/GQDs	27	12	40.16kHz/%RH	20%-90%	[42]
ZnO/Graphene Foam	10	15	33.3 $\Omega$ /%RH	20%-95%	[41]
ZnO/PVP-RGO	12	3	-	15%-95%	[43]

**Table 2, A Comparison table of proposed work & other reported ZnO/Graphene humidity sensors.**

### 4.2 Comparison of proposed work with other reported humidity sensors based on ZnO composite with other 2D materials.

To improve the humidity sensing properties of ZnO, its composite with other 2D materials like MoS<sub>2</sub> [30] and WS<sub>2</sub> [31] etc., has also been reported. Table 3, shows the

performance comparison of this GrF/ZnO composite based humidity sensor to other 2D materials/ZnO composite based humidity sensors. The performance parameters, response time, recovery time, and sensitivity of the proposed sensor make it a better choice for humidity sensing material.

Active material	Response Time (Sec)	Recovery Time (Sec)	Sensitivity (X/%RH)	Range	Reference
ZnO/GrF	0.4	4	7.7 $\mu$ A/%RH	15%-86%	This Work
ZnO/MoS2	1	20	-	11%-95%	[30]
ZnO /WS2	74.51	25.67	101.71fF/% RH	18%-85%	[31]

**Table 3, Comparison table of GrF/ZnO and other 2D materials/ZnO composite based humidity sensors.**

### 4.3 General comparison of proposed work with different graphene composites-based humidity sensors.

Furthermore, Graphene composites with different materials like semiconductors [39], 2D materials [34], polymers [40], metal oxides [32], and biopolymers [37], have been reported for humidity sensors. A detailed comparison between this demonstrated GrF/ZnO composite and various other graphene composite based humidity sensors has been given in Table 4. The sensing performance sets the reported sensor apart from other humidity sensors.

Active material	Response Time (Sec)	Recovery Time (Sec)	Sensitivity (X/%RH)	Range	Reference
ZnO/GrF	0.4	4	7.7 $\mu$ A/%RH	15%-86%	This Work
BP/Graphene	9	30	73 $\Omega$ /%RH	15%-70%	[34]
SiO <sub>2</sub> /PVA/Graphene	24	14.4	2.429kHz/%RH	55%-90%	[39]
Chitosan/GQD	36	3	39.2Hz/%RH	11%-95%	[40]
SnO <sub>2</sub> /RGO	102	6	1604.89 pF/%RH	11%-97%	[32]
Non-woven fabric/GO	8.90	11.76	-	42%-90%	[37]

**Table 4, General comparison of proposed work with different graphene composites-based humidity sensors**

## 5 Conclusion

This work demonstrated an easy, solution-processed, and cost-effective way to make a humidity sensor based on the composite of graphene flower and ZnO. FESEM, EDS, and XRD characterized this composite. It is observed that GrF/ZnO composite has a high surface area porous nanowires type structure, making it a suitable candidate for humidity sensing. Multiple electrical characterizations of prepared humidity sensors were performed at different RH% levels. The proposed humidity sensor has shown an increasing current and a decreasing impedance response w.r.t increase in RH% from 15% to 86%. The demonstrated sensor has shown an ultra-sensitive response, a current change of  $7.7\mu\text{A}/\text{RH}\%$ . Moreover, the sensor revealed a fast response and recovery time as well as offers good stability over the higher humidity. Also, the proposed sensor has shown a measurable current change to even a normal human breath, making it a compelling candidate for health monitoring applications. GrF/ZnO composite has excellent morphological, chemical, and electrical properties that make it a useful candidate for many applications.

## References

- [1] “Industrial Moisture and Humidity Measurement: A Practical Guide - Roland Wernecke, Jan Wernecke - Google Books,” WILEY-VCH, 2014. .
- [2] “Humidity Sensor Market Size, Share & Forecast Report 2019-2025,” KBV Research, 2019. <https://www.kbvresearch.com/humidity-sensor-market/>.
- [3] “Humidity Sensor Market Size, Share | Global Industry Report, 2019-2025,” Grand View Research, 2019. <https://www.grandviewresearch.com/industry-analysis/humidity-sensor-market/toc>.
- [4] A. D. Smith et al., “Resistive graphene humidity sensors with rapid and direct electrical readout,” *Nanoscale*, vol. 7, no. 45, pp. 19099–19109, Dec. 2015, doi: 10.1039/c5nr06038a.
- [5] I. Rahim et al., “Capacitive and resistive response of humidity sensors based on graphene decorated by PMMA and silver nanoparticles,” *Sensors Actuators, B Chem.*, vol. 267, pp. 42–50, Aug. 2018, doi: 10.1016/j.snb.2018.03.069.
- [6] C. Lv et al., “Recent advances in graphene-based humidity sensors,” *Nanomaterials*, vol. 9, no. 3, 2019, doi: 10.3390/nano9030422.
- [7] M. A. Najeeb, Z. Ahmad, and R. A. Shakoor, “Organic Thin-Film Capacitive and Resistive Humidity Sensors: A Focus Review,” *Adv. Mater. Interfaces*, vol. 5, no. 21, pp. 1–19, 2018, doi: 10.1002/admi.201800969.
- [8] M. Cho et al., “Perovskite-Induced Ultrasensitive and Highly Stable Humidity Sensor Systems Prepared by Aerosol Deposition at Room Temperature,” *Adv. Funct. Mater.*, vol. 30, no. 3, p. 1907449, Jan. 2020, doi: 10.1002/adfm.201907449.
- [9] K. Jlassi, S. Mallick, H. Mutahir, Z. Ahmad, and F. Touati, “Synthesis of In Situ Photoinduced Halloysite-Polypyrrole@Silver Nanocomposite for the Potential

Application in Humidity Sensors,” *Nanomaterials*, vol. 10, no. 7, p. 1426, Jul. 2020, doi: 10.3390/nano10071426.

[10] B.-Y. Hwang, W. Du, H.-J. Lee, S. Kang, M. Takada, and J.-Y. Kim, “Stretchable and High-performance Sensor films Based on Nanocomposite of Polypyrrole/SWCNT/Silver Nanowire,” *Nanomaterials*, vol. 10, no. 4, p. 696, Apr. 2020, doi: 10.3390/nano10040696.

[11] M. U. Khan, G. Hassan, and J. Bae, “Bio-compatible organic humidity sensor based on natural inner egg shell membrane with multilayer crosslinked fiber structure,” *Sci. Rep.*, vol. 9, no. 1, Dec. 2019, doi: 10.1038/s41598-019-42337-0.

[12] J. Dai et al., “Ultrafast Response Polyelectrolyte Humidity Sensor for Respiration Monitoring,” *ACS Appl. Mater. Interfaces*, 2019, doi: 10.1021/acsami.8b18904.

[13] A. M. Soomro, F. Jabbar, M. Ali, J. W. Lee, S. W. Mun, and K. H. Choi, “All-range flexible and biocompatible humidity sensor based on poly lactic glycolic acid (PLGA) and its application in human breathing for wearable health monitoring,” *J. Mater. Sci. Mater. Electron.*, vol. 30, no. 10, pp. 9455–9465, May 2019, doi: 10.1007/s10854-019-01277-1.

[14] N. Horzum, D. Taşçıoğlu, S. Okur, and M. M. Demir, “Humidity sensing properties of ZnO-based fibers by electrospinning,” *Talanta*, vol. 85, no. 2, pp. 1105–1111, Aug. 2011, doi: 10.1016/j.talanta.2011.05.031.

[15] M. U. Khan, G. Hassan, M. Awais, and J. Bae, “All printed full range humidity sensor based on Fe<sub>2</sub>O<sub>3</sub>,” *Sensors Actuators, A Phys.*, vol. 311, p. 112072, Aug. 2020, doi: 10.1016/j.sna.2020.112072.



- [16] M. Velumani, S. R. Meher, and Z. C. Alex, "Composite metal oxide thin film based impedometric humidity sensors," *Sensors Actuators, B Chem.*, vol. 301, p. 127084, Dec. 2019, doi: 10.1016/j.snb.2019.127084.
- [17] A. Farzaneh, A. Mohammadzadeh, M. D. Esrafil, and O. Mermer, "Experimental and theoretical study of TiO<sub>2</sub> based nanostructured semiconducting humidity sensor," *Ceram. Int.*, vol. 45, no. 7, pp. 8362–8369, May 2019, doi: 10.1016/j.ceramint.2019.01.144.
- [18] N. Irawati, H. A. Rahman, H. Ahmad, and S. W. Harun, "A PMMA microfiber loop resonator based humidity sensor with ZnO nanorods coating," *Meas. J. Int. Meas. Confed.*, vol. 99, pp. 128–133, Mar. 2017, doi: 10.1016/j.measurement.2016.12.021.
- [19] L. Gu et al., "Humidity sensors based on ZnO/TiO<sub>2</sub> core/shell nanorod arrays with enhanced sensitivity," *Sensors Actuators, B Chem.*, vol. 159, no. 1, pp. 1–7, Nov. 2011, doi: 10.1016/j.snb.2010.12.024.
- [20] H. Dai, N. Feng, J. Li, J. Zhang, and W. Li, "Chemiresistive humidity sensor based on chitosan/zinc oxide/single-walled carbon nanotube composite film," *Sensors Actuators, B Chem.*, vol. 283, pp. 786–792, Mar. 2019, doi: 10.1016/j.snb.2018.12.056.
- [21] W. Wang et al., "Humidity sensor based on LiCl-doped ZnO electrospun nanofibers," *Sensors Actuators, B Chem.*, vol. 141, no. 2, pp. 404–409, Sep. 2009, doi: 10.1016/j.snb.2009.06.029.
- [22] S. Yu, H. Zhang, C. Chen, and C. Lin, "Investigation of humidity sensor based on Au modified ZnO nanosheets via hydrothermal method and first principle," *Sensors Actuators, B Chem.*, vol. 287, pp. 526–534, May 2019, doi: 10.1016/j.snb.2019.02.089.
- [23] A. S. Ismail et al., "Enhanced humidity sensing performance using Sn-Doped ZnO nanorod Array/SnO<sub>2</sub> nanowire heteronetwork fabricated via two-step solution

immersion,” *Mater. Lett.*, vol. 210, pp. 258–262, Jan. 2018, doi: 10.1016/j.matlet.2017.09.040.

[24] S. P. Chang et al., “A ZnO nanowire-based humidity sensor,” *Superlattices Microstruct.*, vol. 47, no. 6, pp. 772–778, Jun. 2010, doi: 10.1016/j.spmi.2010.03.006.

[25] I. Y. Y. Bu and C. C. Yang, “High-performance ZnO nanoflake moisture sensor,” *Superlattices Microstruct.*, vol. 51, no. 6, pp. 745–753, Jun. 2012, doi: 10.1016/j.spmi.2012.03.009.

[26] H. H. M. Yusof et al., “Low-Cost Integrated Zinc Oxide Nanorod-Based Humidity Sensors for Arduino Platform,” *IEEE Sens. J.*, vol. 19, no. 7, pp. 2442–2449, Apr. 2019, doi: 10.1109/JSEN.2018.2886584.

[27] A. Erol, S. Okur, B. Comba, Ö. Mermer, and M. Ç. Arikian, “Humidity sensing properties of ZnO nanoparticles synthesized by sol-gel process,” *Sensors Actuators, B Chem.*, vol. 145, no. 1, pp. 174–180, Mar. 2010, doi: 10.1016/j.snb.2009.11.051.

[28] N. F. Hsu, M. Chang, and C. H. Lin, “Synthesis of ZnO thin films and their application as humidity sensors,” in *Microsystem Technologies*, Nov. 2013, vol. 19, no. 11, pp. 1737–1743, doi: 10.1007/s00542-013-1830-z.

[29] G. Hassan, J. Bae, C. H. Lee, and A. Hassan, “Wide range and stable ink-jet printed humidity sensor based on graphene and zinc oxide nanocomposite,” *J. Mater. Sci. Mater. Electron.*, vol. 29, no. 7, pp. 5806–5813, Apr. 2018, doi: 10.1007/s10854-018-8552-z.

[30] L. Ze, G. Yueqiu, L. Xujun, and Z. Yong, “MoS<sub>2</sub>-modified ZnO quantum dots nanocomposite: Synthesis and ultrafast humidity response,” *Appl. Surf. Sci.*, vol. 399, pp. 330–336, Mar. 2017, doi: 10.1016/j.apsusc.2016.12.034.

- [31] M. A. Dwiputra, F. Fadhila, C. Imawan, and V. Fauzia, “The enhanced performance of capacitive-type humidity sensors based on ZnO nanorods/WS<sub>2</sub> nanosheets heterostructure,” *Sensors Actuators, B Chem.*, vol. 310, p. 127810, May 2020, doi: 10.1016/j.snb.2020.127810.
- [32] D. Zhang, H. Chang, P. Li, R. Liu, and Q. Xue, “Fabrication and characterization of an ultrasensitive humidity sensor based on metal oxide/graphene hybrid nanocomposite,” *Sensors Actuators, B Chem.*, vol. 225, pp. 233–240, Mar. 2016, doi: 10.1016/j.snb.2015.11.024.
- [33] S. Ali, A. Hassan, G. Hassan, J. Bae, and C. H. Lee, “All-printed humidity sensor based on gmethyl-red/methyl-red composite with high sensitivity,” *Carbon N. Y.*, vol. 105, pp. 23–32, Aug. 2016, doi: 10.1016/j.carbon.2016.04.013.
- [34] D. T. Phan, I. Park, A. R. Park, C. M. Park, and K. J. Jeon, “Black P/graphene hybrid: A fast response humidity sensor with good reversibility and stability,” *Sci. Rep.*, vol. 7, no. 1, pp. 1–7, 2017, doi: 10.1038/s41598-017-10848-3.
- [35] C. Chen, X. Wang, M. Li, Y. Fan, and R. Sun, “Humidity sensor based on reduced graphene oxide/lignosulfonate composite thin-film,” *Sensors Actuators, B Chem.*, vol. 255, pp. 1569–1576, Feb. 2018, doi: 10.1016/j.snb.2017.08.168.
- [36] P. He et al., “Fully printed high performance humidity sensors based on two-dimensional materials,” *Nanoscale*, vol. 10, no. 12, pp. 5599–5606, Mar. 2018, doi: 10.1039/c7nr08115d.
- [37] Y. Wang, L. Zhang, Z. Zhang, P. Sun, and H. Chen, “High-Sensitivity Wearable and Flexible Humidity Sensor Based on Graphene Oxide/Non-Woven Fabric for Respiration Monitoring,” *Langmuir*, vol. 36, no. 32, pp. 9443–9448, Aug. 2020, doi: 10.1021/acs.langmuir.0c01315.

- [38] Muhammad Tariq Saeed Chani et al., “Humidity Sensor Based on Orange Dye and Graphene Solid Electrolyte Cells,” *Russ. J. Electrochem.*, vol. 55, no. 12, pp. 1391–1396, Dec. 2019, doi: 10.1134/S1023193519120036.
- [39] Y. Su et al., “Surface acoustic wave humidity sensor based on three-dimensional architecture graphene/PVA/SiO<sub>2</sub> and its application for respiration monitoring,” *Sensors Actuators, B Chem.*, vol. 308, p. 127693, Apr. 2020, doi: 10.1016/j.snb.2020.127693.
- [40] P. Qi, T. Zhang, J. Shao, B. Yang, T. Fei, and R. Wang, “A QCM humidity sensor constructed by graphene quantum dots and chitosan composites,” *Sensors Actuators, A Phys.*, vol. 287, pp. 93–101, Mar. 2019, doi: 10.1016/j.sna.2019.01.009.
- [41] M. Morsy, M. Ibrahim, Z. Yuan, and F. Meng, “Graphene Foam Decorated with ZnO as a Humidity Sensor,” *IEEE Sens. J.*, vol. 20, no. 4, pp. 1721–1729, Feb. 2020, doi: 10.1109/JSEN.2019.2948983.
- [42] J. Wu et al., “Ultrathin Glass-Based Flexible, Transparent, and Ultrasensitive Surface Acoustic Wave Humidity Sensor with ZnO Nanowires and Graphene Quantum Dots,” *ACS Appl. Mater. Interfaces*, vol. 12, no. 35, pp. 39817–39825, Sep. 2020, doi: 10.1021/acsami.0c09962.
- [43] H. Yang et al., “Stable and Fast-Response Capacitive Humidity Sensors Based on a ZnO Nanopowder/PVP-RGO Multilayer,” *Sensors*, vol. 17, no. 10, p. 2415, Oct. 2017, doi: 10.3390/s17102415.
- [44] D. Zhang, J. Liu, and B. Xia, “Layer-by-Layer Self-Assembly of Zinc Oxide/Graphene Oxide Hybrid Toward Ultrasensitive Humidity Sensing,” *IEEE Electron Device Lett.*, vol. 37, no. 7, pp. 916–919, Jul. 2016, doi: 10.1109/LED.2016.2565728.

- [45] M. Zafar, J. Y. Yun, and D. H. Kim, "Improved inverted-organic-solar-cell performance via sulfur doping of ZnO films as electron buffer layer," *Mater. Sci. Semicond. Process.*, vol. 96, pp. 66–72, Jun. 2019, doi: 10.1016/j.mssp.2019.01.046.
- [46] M. Z. Toe et al., "Effect of ZnO seed layer on the growth of ZnO nanorods on silicon substrate," in *Materials Today: Proceedings*, Jan. 2019, vol. 17, pp. 553–559, doi: 10.1016/j.matpr.2019.06.334.
- [47] S. N. Chen, M. Z. Huang, Z. H. Lin, and C. P. Liu, "Enhancing charge transfer for ZnO nanorods based triboelectric nanogenerators through Ga doping," *Nano Energy*, vol. 65, p. 104069, Nov. 2019, doi: 10.1016/j.nanoen.2019.104069.
- [48] X. Li, Z. Wang, Y. Qiu, Q. Pan, and P. Hu, "3D graphene/ZnO nanorods composite networks as supercapacitor electrodes," *J. Alloys Compd.*, vol. 620, pp. 31–37, Jan. 2015, doi: 10.1016/j.jallcom.2014.09.105.
- [49] R. Cai et al., "3D graphene/ZnO composite with enhanced photocatalytic activity," *Mater. Des.*, vol. 90, pp. 839–844, Jan. 2016, doi: 10.1016/j.matdes.2015.11.020.